

A Flip-Chip-Packaged and Fully Integrated 60 GHz CMOS Micro-Radar Sensor for Heartbeat and Mechanical Vibration Detections

Te-Yu Jason Kao, Austin Ying-Kuang Chen*, Yan Yan, Tze-Min Shen, and Jenshan Lin

Department of ECE, University of Florida, Gainesville, FL 32611, USA

*Now with Skyworks Solutions, Newbury Park, CA 91320, USA

Abstract — A 60 GHz micro-radar in 90 nm CMOS for non-contact vital sign and small vibration detections was designed and tested. A quadrature receiver embedded in the indirect up- and down-conversion architecture solves the null detection point issue and increases the robustness of the millimeter wave system. In the 60 GHz core, lumped-element-modeled passive components are extensively used to achieve a compact layout (0.73 mm^2), and a 36 dB down-conversion gain at 55 GHz. Using low-cost single-patch PCB antennas, flip-chip packaging of the CMOS chip demonstrates high level of system integration. First pass success is achieved as the human heartbeat and a small mechanical vibration with a displacement of $20 \text{ }\mu\text{m}$ can be detected at 0.3 m away. With a roughly one-tenth patch antenna size compared to previously reported works, the 60 GHz CMOS integrated micro-radar can be readily embedded in various portable devices to detect vary small vibrations and used for many applications.

Index Terms — CMOS, Doppler radar, flip chip, millimeter wave integrated circuits, medical signal detection, patch antennas, sensor systems, frequency measurement.

I. INTRODUCTION

Recent progress on non-contact vital sign and vibration detections has been made based on microwave Doppler radar system [1]-[4]. Double-sideband architecture with frequency tuning [3] is used to eliminate the null detection point which occurs every $\lambda/4$ from the radar. Moreover, a 5.8 GHz CMOS quadrature receiver with complex signal demodulation (CSD) solving the null point issue was developed in [1] [2] for non-contact vital sign detection.

The wavelength (λ) of radar signal is one of the key factors in determining the sensitivity to small vibration. A 94 GHz CMOS Doppler transceiver with horn antennas potentially for the detection of very small movement was demonstrated [5]. The use of millimeter-wave (mm-wave) radar signal introduces more design requirement for the low-loss transition between the chip and antennas, similar to that of the mm-wave communication systems which have drawn increasing attention in the recent years.

While several mm-wave packaging techniques have been developed in [6]-[7], this paper demonstrates a standard flip-chip integration of a 60 GHz CMOS chip and PCB patch antennas without any extra supporting

structure to horizontally align the chip and antennas. The low-cost PCB patch antennas with a better performance compared to an on-chip counterpart can be used to realize high level of mm-wave system integration. In addition, with a roughly one-tenth patch antenna size and lightweight compared to the previous works at 6 GHz, the 60 GHz CMOS flip-chip-packaged sensor system can be readily embedded into one of the smartphone functions, for example, making it a pervasive first-aid tool for non-contact vital sign monitoring, or also be applied to a large sensor network.

II. SYSTEM DESIGN

Fig. 1 shows the top view of the system including the CMOS radar chip (0.96 mm by 2.35 mm) and two PCB patch antennas on RT/duroid 5870 laminate (31.3 mm by 45 mm) for transmitting (TX) and receiving (RX). RF pads on the chip and metal traces on the laminate (zoom-in area) are designed for mm-wave flip-chip integration.

The integrated transmitter containing two VCOs, an up-conversion mixer, a balun, and a driver is designed to transmit an unmodulated 60 GHz continuous wave (CW) signal through the TX antenna. The signal is reflected and phase modulated by a small vibration of the target due to Doppler effect, and then received by the RX antenna. For the integrated receiver, the weak received signal is amplified by a 60 GHz high-gain LNA and down-converted by the same VCOs. Since the same VCOs are used for TX and RX and the phase noises are correlated for short distance detection, this range correlation effect [4] results in significant reduction of VCO phase noise at radar baseband output and thus free-running VCOs can be adopted. The indirect down-conversion topology using an active and two passive mixers was designed to minimize the flicker noise presented in the baseband (0-2 Hz), which will be explained in the following section. The existence of IF also improves the robustness of the system by compensating the possible RF drift due to mm-wave circuit modeling uncertainty, and provides more flexibility to optimize the system performance.

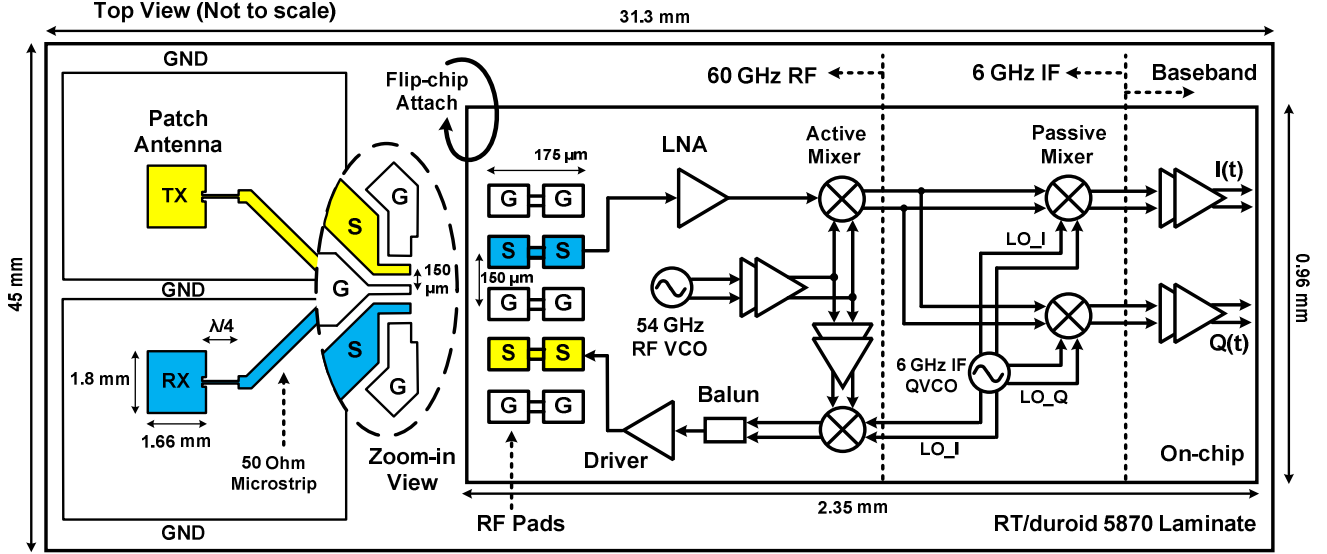


Fig. 1. System block diagram illustrating CMOS micro-radar chip, PCB TX and RX patch antennas, and flip-chip integration.

To eliminate null detection point issue without extra frequency tuning [3], the quadrature (I/Q) channels with two sets of baseband amplifiers are implemented, enabling the baseband outputs $I(t)$ and $Q(t)$ to be directly sampled for CSD in software [2]. Quadrature LO is generated by the 6 GHz ring oscillator at IF stage and eliminates the need for a quadrature VCO at 60 GHz RF.

III. COMPONENT DESIGN

A. Transceiver Circuits

In the gain budget analysis, the calculated maximum received power by the RX antenna for an infinitely large perfect reflector at 2 m away is -64 dBm. This assumes the transmitted power is 0 dBm and the TX and RX antennas have 5 dB gain each. The actual received power should be lower due to the actual smaller reflection area. Thus, a high-gain first stage of the receiver was targeted. However, the scaled CMOS technology poses several challenges such as thin metal layers and high loss through substrate, which have to be taken into account during the mm-wave passive components design. A five-stage cascode LNA was designed to provide a gain of 40 dB at 60 GHz while consuming 50 mW. Lumped-element-modeled, L-shaped inductors are used extensively to achieve a compact LNA layout (0.26 mm^2).

To minimize the flicker noise at baseband, two passive IF mixers with large transistor sizes are used for I/Q channels [1]. The single-balanced active RF mixer with a simulated gain of 0 dB serves as single-ended to differential conversion and form the indirect down-conversion architecture. Similar to the design method in

[8], a 54 GHz LC cross-coupled VCO with LO distribution buffer network is implemented to drive the up- and down-conversion mixers. Since the range correlation effect relaxes the phase noise requirement, the 6 GHz quadrature ring oscillator is adopted to provide a quadrature LO with a wide tuning range (2 GHz to 8 GHz). Fig. 2 shows the microphotograph of the micro-radar in 90 nm CMOS technology. The area reduction of the prototype chip is limited by the number of DC pads for bias optimization. The 60 GHz core is 0.73 mm^2 .

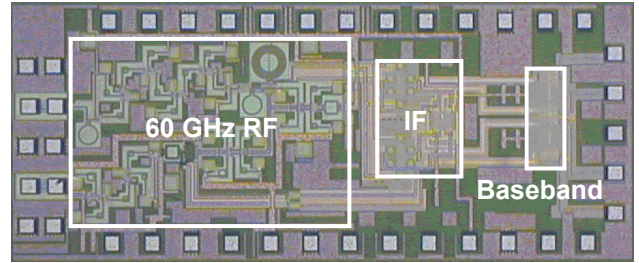


Fig. 2. Microphotograph of the 60 GHz CMOS micro-radar.

B. Antenna and Flip-Chip Package

The TX and RX patch antennas were fabricated on a 5-mil-thick RT/duroid 5870 laminate providing a gain of 6 dB each, and the angle between two 50 feedlines were designed to be 90° for better TX/RX isolation to reduce DC offset at baseband. A FR4 laminate was attached to the backside to support the soft 5870 laminate. The pitches of the RF pads on chip and the traces on PCB were designed to match to $150 \mu\text{m}$ for two reasons. First, the $150 \mu\text{m}$ pitch means 3 mil trace width and spacing on the PCB, which is the resolution limit of the etching process. Second, $150 \mu\text{m}$ is compatible with the pitch of V-band

RF probes, such that the antennas can be designed and tested after measuring the optimal operating frequency of the chip. In the flip-chip process, solder bumps were placed on the chip pads and designed to be around 30 μm in height and 50 μm in diameter after reflow. Double-column RF pads are used to further reduce the series inductance and resistance. In the electromagnetic (EM) simulation, this flip-chip transition structure shows very limited impact on the series inductance and return loss (S_{11}) even at 60 GHz, and thus is adopted in the system.

IV. EXPERIMENT RESULTS

A. Millimeter-wave Transceiver

A separate test structure which duplicates the 60 GHz RF core in Fig. 1 was measured. At a total 190 mW power consumption (1.2 V power supply), the receiver provides more than 30 dB down-conversion gain from 52 GHz to 56.5 GHz as plotted in Fig. 3. The peak down-conversion gain is 36 dB at 55 GHz with the RF VCO operating at 48.4 GHz. The OP1dB of the receiver is -5.7 dBm. For the TX, the transmitted power at antenna port is around 1.5 dBm at 55 GHz. The OP1dB of the transmitter is measured to be -0.3 dBm.

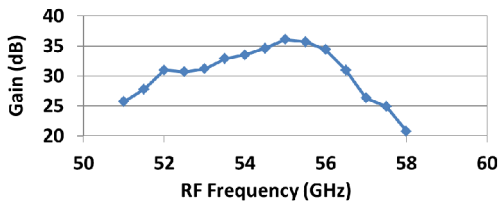


Fig. 3. Measured down-conversion gain (RF to IF) versus frequency. The RF input power was set at -60 dBm to emulate the weak reflected signal received by the RX antenna.

B. Non-contact Heartbeat Detection

Fig. 4 shows the integrated system used to detect heartbeat and mechanical vibration. It was pasted on a vertically placed cardboard to face the target. The directly sampled heartbeat signal in Fig. 5 (a) and (b) was obtained from a person sitting on a chair with his chest wall 0.3 m in front of the antennas. The breath was held to avoid the interference by the harmonics of respiration signal. The result clearly shows the robustness of the I/Q topology to avoid the null detection points, which occur every 1.25 mm ($\lambda/4$) from the radar. At $t = 0 \sim 7$ sec, Q channel was around the optimal point while I channel was near the null point. However, the target entered the null point of Q channel after $t = 9$ sec due to some slight body movement, and I channel started to take over the detection. Fig. 5 (c) shows the spectrum of detected signal and the heartbeat rate at 69 beats/minute (BPM) after the CSD, which

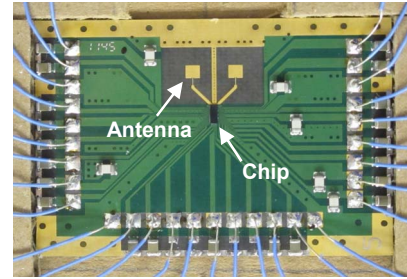


Fig. 4. The integrated system including the chip, antennas, and bypass capacitors on the PCB, and the wires are connected to DC power supplies. The PCB weights less than 5 grams.

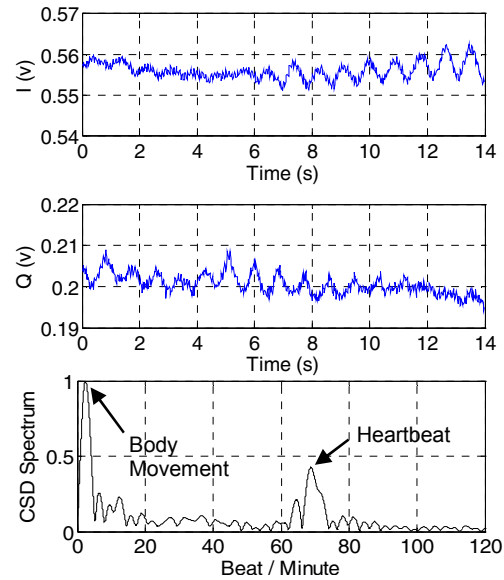


Fig. 5. (a) and (b) Baseband IQ outputs of heartbeat signal sampled and displayed by the oscilloscope. (c) CSD spectrum showing heartbeat rate at 69 BPM.

agrees with the result of human counting. The Doppler frequency shift due to body movement also shows up in the spectrum. The total power consumption of the system is 377 mW at 1.2 V power supply.

The total baseband output noise of the system is band-limited by the sampling rate of the baseband ADC. In this case (Fig. 5) the sampling rate is 50 Hz and the measured baseband noise voltage is around 1 mV_{rms}, corresponding to a baseband SNR around 5 (14 dB). This result is consistent with [1] showing that even the noise figure of the system could be high around the band of interest due to the large CMOS flicker noise, the vital sign detection is still achievable by proper design of the system.

C. Detection of Small Mechanical Vibration

To explore the detection range and resolution of small vibration, a 0.15 m by 0.15 m metal plate was attached to a Zaber T-LA60A-S actuator and placed at a distance D

from the radar. A 1 Hz mechanical vibration was generated by the actuator with displacement A . At $D = 0.3$ m, A was varied and the received CSD spectrum was normalized by the largest displacement ($A = 1$ mm) as presented in Fig. 6 (a). The figure shows the vibration frequency (1 Hz) can still be detected when A is as small as 0.02 mm. Fig 6 (b) displays a more complete comparison through the same normalization. Two observations are made from the plot. First, the received CSD spectrum peak decreases with distance as expected. A small vibration with $A = 0.2$ mm can be detected at $D = 2.1$ m away. Second, at a fixed distance, the sensitivity to “displacement change” increases when the vibration is getting smaller. For example, at $D = 0.3$ m, as A is reduced by half from 1 mm to 0.5 mm, the CSD spectrum peak drops about 18% (1 to 0.82); however, as A is reduced by half from 0.2 mm to 0.1 mm, the drop of CSD spectrum peak increases to 42% (0.53 to 0.31). This implies the detection has an optimal range of target vibration displacement which is worth to be investigated further.

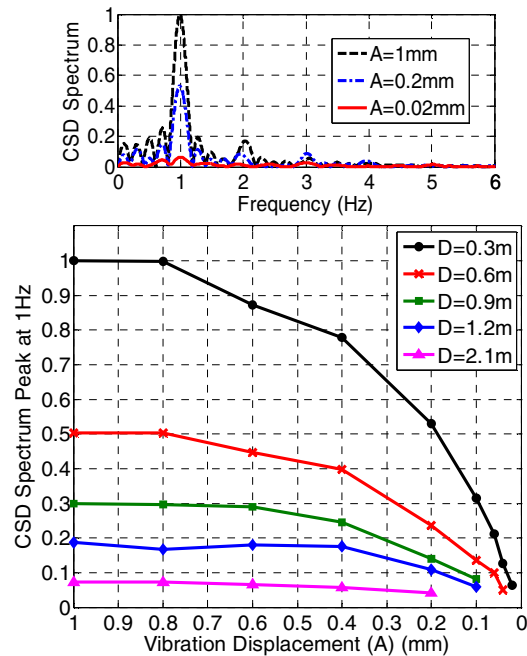


Fig. 6. (a) Spectrum of radar-detected 1 Hz mechanical vibration with different vibration displacement A at 0.3 m away (b) CSD spectrum peak at 1 Hz versus vibration displacement A at various distances. All the data points are normalized to the largest CSD spectrum peak at $A = 1$ mm, $D = 0.3$ m.

V. CONCLUSION

A 60 GHz radar sensor chip fabricated in UMC 90 nm CMOS process was integrated with two on-board patch antennas by flip-chip packaging. Measurement data

demonstrated the successful detections of human heartbeat and small mechanical vibration. The increased sensitivity to the change of vibration displacement was observed when the displacement was getting smaller. The compact and lightweight integrated micro-radar can be embedded in portable equipment for healthcare monitoring, vibration sensing, and many other applications.

ACKNOWLEDGEMENT

The authors would like to acknowledge the single-die bumping and flip-chip service sponsored by Mr. Terence Collier from CVInc, Richardson, Texas, USA. The authors also acknowledge the 90 nm CMOS chip fabrication by United Microelectronics Corporation (UMC), HsinChu, Taiwan, and the microwave PCBs provided by Rogers Corporation, Rogers, CT, USA.

REFERENCES

- [1] C. Li, X. Yu, C. Lee, L. Ran, and J. Lin, “High-sensitivity software configurable 5.8 GHz radar sensor receiver chip in 0.13 μ m CMOS for non-contact vital sign detection,” *IEEE Trans. Microwave Theory & Tech.*, vol. 58, issue 5, pp. 1410-1419, May 2010.
- [2] C. Li, and J. Lin, “Complex signal demodulation and random body movement cancellation techniques for non-contact vital sign detection,” *IEEE MTT-S Int. Microw. Symp. Dig., Atlanta*, pp. 567-570, June 2008.
- [3] Y. Xiao, J. Lin, O. Boric-Lubecke, and V. M. Lubecke, “Frequency tuning technique for remote detection of heartbeat and respiration using low-power double-sideband transmission in Ka-band,” *IEEE Trans. Microwave Theory & Tech.*, vol. 54, pp. 2023-2032, May 2006.
- [4] A. D. Droitcour, O. Boric-Lubecke, V. M. Lubecke, J. Lin, and G. T. A. Kovac, “Range correlation and I/Q performance benefits in single-chip silicon Doppler radars for noncontact cardiopulmonary monitoring,” *IEEE Trans. Microwave Theory & Tech.*, vol. 52, no.3, pp. 838-848, Mar. 2004.
- [5] E. Laskin, M. Khanpour, S. T. Nicolson, A. Tomkins, P. Garcia, A. Cathelin, D. Belot, and S. P. Voinigescu, “Nanoscale CMOS transceiver design in the 90-170 GHz range,” *IEEE Trans. Microwave Theory & Tech.*, vol. 57, pp. 3477-3490, Dec. 2009.
- [6] J. Lee, Y. Chen, and Y. Huang, “A low-power low-cost fully-integrated 60-GHz transceiver system with OOK modulation and on-board antenna assembly,” *IEEE J. Solid State Circuits*, vol. 45, no. 2, pp.264-275, Feb. 2010.
- [7] S. Reynolds, B. Floyd, U. Pfeiffer, T. Beukema, J. Grzyb, C. Haymes, B. Gaucher, and M. Soyuer, “A silicon 60 GHz receiver and transmitter chipset for broadband communications,” *IEEE J. Solid State Circuits*, vol. 41, no. 12, pp. 2820-2831, Dec 2006.
- [8] C. Cao and K. K. O, “Millimeter-wave voltage-controlled oscillators in 0.13- μ m CMOS technology,” *IEEE J. Solid State Circuits*, vol. 41, no. 6, pp. 1297-1304, June 2006.